

ARTICLES

Temperature dependence of the elastic constants of LiKSO₄ through a first-order structural phase transition

F. Willis and R. G. Leisure

Department of Physics, Colorado State University, Fort Collins, Colorado 80523

T. Kanashiro

Department of Physics, Tokushima University, Tokushima, Japan

(Received 26 April 1996)

Resonant ultrasound spectroscopy has been used to measure the complete set of elastic constants of LiKSO₄ over the temperature range of 200 to 300 K including both the hexagonal room temperature phase and the lower temperature trigonal phase. Large step changes are observed in all the elastic constants, except C_{13} , at 213 K on cooling and at 243 K on warming. These step changes are associated with the hexagonal/trigonal crystallographic phase transition. The bulk modulus is approximately 15% higher in the trigonal phase than in the hexagonal phase. The hexagonal-phase elastic constants exhibit very little temperature dependence while the trigonal-phase elastic constants show a stronger dependence on temperature. The transitions are noted to be quite sluggish, taking a few hours to equilibrate. The results are described in terms of a Landau-type free energy expansion using two Ising-like order parameters with strong coupling between the two parameters. Biquadratic coupling between the order parameters and strains is shown to account for the step changes in the elastic constants as well as the temperature dependence in the trigonal phase. Coupling linear in the strains is shown to be insufficient to explain the results. [S0163-1829(96)02237-0]

I. INTRODUCTION

Sulfate compounds of the form $ABSO_4$ ($A, B = \text{Li, Na, K, Cs, Rb, Ag, H, and NH}_4$) have received much study in recent years¹ due to their unusual physical properties and a rich sequence of phase transitions. The differences between the various phases are largely associated with the SO_4 tetrahedra. At high temperatures the SO_4 tetrahedra undergo rapid rotation resulting in a relatively high-symmetry phase. These phases are often superionic conductors due to the high mobility of the cations. This high mobility has been attributed to an interaction between the cations and the rotating sulfate ions.² As the temperature is lowered the rapid rotation freezes out and various tilts of the SO_4 tetrahedra give rise to a series of phase transitions. Lithium potassium sulfate (LiKSO₄) has been especially studied because large single crystals are relatively easy to grow, the material is stable, and the crystals survive first-order structural phase transitions without breaking. Although the structure of LiKSO₄ has been the subject of numerous investigations,³⁻¹¹ there is still controversy concerning some of the phases. Much of the problem stems from the fact that the phase transitions in LiKSO₄ are first order. Single crystals are easy to grow at room temperature, but complicated domain structures or mixed phases often appear after the crystal undergoes a first order phase transition.¹² These mixed phases lead to much controversy over the actual crystalline structure.

The focus of the present study is on the transition between the room temperature phase and the first phase appearing as the temperature is lowered from room temperature. This

transition occurs at approximately 210 K on cooling and 240 K on warming. The structure of the room temperature phase seems firmly established as hexagonal ($P6_3$), but the structure of the lower temperature phase has been difficult to determine. Early neutron diffraction measurements¹³ showed a mixture of $P6_3$ and $P31c$ phases when LiKSO₄ is cooled below 205 K. More recent measurements¹⁴ support the trigonal $P31c$ phase below room temperature. A complication of the transition occurring near 210 K on cooling is its sluggish nature. There are reports of the transition taking place over time frames ranging from several hours to more than a day.¹⁴⁻¹⁶

The sequence of low temperature phase transitions in LiKSO₄ has been studied by a variety of methods,^{12,14,17-21} including four studies of the elastic constants immediately below room temperature.^{15,16,22,23} Three of the elastic constant studies were by means of Brillouin scattering and one utilized a low-frequency torsion pendulum. In general, the various experiments are not in agreement with each other. The two experiments which measured the elastic constant C_{66} both reported a softening as the crystal transformed into the trigonal phase. However, the results for other elastic constants are qualitatively different for different experiments, perhaps due to time-dependent effects.

Despite experimental difficulties in dealing with LiKSO₄, it remains a very interesting system to study. The presence of a hexagonal to trigonal transition just below room temperature provides an excellent opportunity to study a low symmetry, first-order transition. Second order transitions have received much interest in the past, in large part due to an

interest in studying systems exhibiting soft modes.²⁴ The soft mode model requires the restoring force to vanish at the transition temperature, but this is not true in the case of first-order transitions. Even though first-order transitions are much more numerous than second-order transitions, second-order transitions have received much more attention. In particular, the elastic properties of a number of materials undergoing second-order transitions have been studied through the temperature range corresponding to the transition.^{25,26} The situation is quite different regarding the elastic properties of materials undergoing first-order transitions. It is rare that elastic constants are measured through the transition region, although this has been achieved in a few cases for martensitic transitions in alloys.^{27–32} Other than studies of the martensitic transition with a cubic parent phase, there appear to be few detailed studies of elastic constants near a first-order phase transition.

Resonant ultrasound spectroscopy (RUS) (Refs. 33–35) offers an attractive method for studying first-order phase transitions for several reasons. RUS is a technique that allows the simultaneous determination of the complete set of elastic constants for a material. In addition, RUS works quite well with samples as small as 1 mm³, which is more than two orders of magnitude smaller than samples volumes used in typical ultrasonic or Brillouin scattering experiments. This ability to use a small single crystal for the study means there is a much better chance to avoid domain formation during the phase transition. An additional feature of RUS is that there is no need to attach ultrasonic transducers to the sample. A parallelepiped is simply balanced along a body diagonal between two ultrasonic transducers. The absence of a bonding agent between the transducers and crystal also eliminates a strain being applied to the surface of the crystal due to the different thermal expansions of the two materials.

Elastic constants, being the second derivative of the free energy with respect to strain, are usually strongly affected by structural phase transitions. In view of the disagreement in the literature over the values of the elastic constants near the hexagonal/trigonal transition in LiKSO₄, and also in view of the possibility of obtaining the complete set of elastic constants on both sides of the transition using RUS, we report below the results of elastic constant measurements in this material over the temperature range of 200–300 K.

II. EXPERIMENTAL DETAILS

The LiKSO₄ single crystal used for this study was grown by slow evaporation of an equimolar aqueous solution of Li₂SO₄·H₂O(99.9%) and K₂SO₄(99%). The solution was allowed to evaporate at room temperature and the crystal grown over a period of approximately one month. The crystal used in this study grew in the shape of a hexagonal prism with a clearly defined sixfold axis. The orientation of the crystal was determined from the morphology based on the description by Pimenta *et al.*³⁶ An initial optical examination of the crystal revealed excellent clarity with no signs of the cloudy regions common in this material. Examination with polarizing filters and a low power microscope showed the crystal was uniformly optically active. No defects were observed.

Two of the original crystal surfaces were used for orien-

tation during sample preparation. A rough cube approximately 2 mm on each side was cut from the crystal. Two of the faces of the cube were the top ([001]) and one of the side facets ([100]) of the crystal. These two perpendicular surfaces were used to polish the cube into a parallelepiped suitable for measurement with RUS. The final dimensions of the parallelepiped were 0.1349×0.1528×0.1361 cm³. For consistency with previous publications, the density was assumed to be 2.383 g/cm³.

RUS is a technique for determining the elastic constants of materials by measuring a set of macroscopic resonant frequencies.^{37–39} A sample of specified shape is balanced between two ultrasonic transducers. One transducer is used to excite vibrations in the sample at a specific frequency. The resulting vibration induces a voltage on the second transducer which is amplified and detected by a digital voltmeter. The frequency of the driving transducer is incremented and the process repeated until a range of frequencies has been scanned. A more detailed scan is then made in the region of each of the resonant frequencies. The density, shape, dimensions and estimates for the elastic constants are used to calculate a set of resonant frequencies. This set of calculated frequencies is compared to the set of experimentally determined frequencies and corrections to the elastic constants are made. The iterations are repeated until a suitable fit between the calculated frequencies and measured frequencies is achieved.

The temperature was controlled through the use of a gas flow cryostat. The temperature was typically held to within ±0.04 K of the target temperature for approximately 30 min while the data were being taken. Except near the transitions, the temperature was changed by approximately 0.2 K/min. The system was allowed to stabilize at each temperature for approximately 30 min before data were taken. The temperature cycle from room temperature to 200 K and back to room temperature required 85 h. Approximately 3 h was spent in the immediate vicinity (±0.5 K) of each transition.

III. RESULTS

Representative RUS scans showing the lowest five resonances in both the hexagonal and trigonal phases of LiKSO₄ are presented in Fig. 1. As can be seen, there is a large difference in the resonant frequencies between the two phases. The lowest resonant frequency for a sample of the size and shape described above is about 0.800 MHz in the hexagonal phase. It is only slightly temperature dependent, being 0.795 MHz at 296 K and increasing to 0.803 MHz at 215 K. As the sample is cooled through the transition at 213 K, the resonant frequencies are observed to decrease sharply. For example, the frequency of the lowest resonance dropped abruptly by more than a factor of 2 and continued decreasing slowly for 2–3 h. The temperature was maintained to within ±0.5 K of the temperature at which the transition was first observed until the resonant frequencies stabilized. The crystal was then cooled to 200 K and allowed to stabilize for an additional 6 h. The temperature dependence of the resonant frequencies in the trigonal phase is greater than in the hexagonal phase. The lowest resonant frequency is 0.3518 MHz

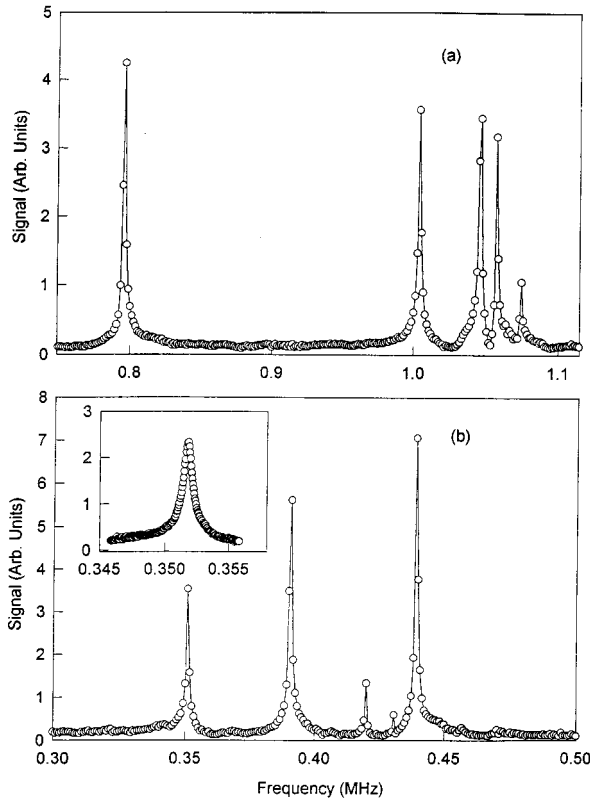


FIG. 1. Representative RUS spectra for a LiKSO_4 parallelepiped in the hexagonal (a) and trigonal (b) phases.

at 204 K and increases to 0.4426 MHz at 240 K. At 243 K on warming the frequencies return abruptly to the hexagonal phase values.

The elastic constant matrix can be represented by

$$C = \begin{pmatrix} C_{11} & C_{12} & C_{13} & C_{14} & -C_{25} & 0 \\ C_{12} & C_{11} & C_{13} & -C_{14} & C_{25} & 0 \\ C_{13} & C_{13} & C_{33} & 0 & 0 & 0 \\ C_{14} & -C_{14} & 0 & C_{44} & 0 & C_{25} \\ -C_{25} & C_{25} & 0 & 0 & C_{44} & C_{14} \\ 0 & 0 & 0 & C_{25} & C_{14} & C_{66} \end{pmatrix}, \quad (1)$$

$$C_{66} = \frac{1}{2} (C_{11} - C_{12}),$$

where $C_{14} = C_{25} = 0$ for the hexagonal case. Thus there are five independent elastic constants for hexagonal symmetry. For the most general trigonal case, there are seven independent elastic constants. Federov⁴⁰ shows that a rotation of the crystal about the c -axis can be made such that either $C_{14} \neq 0$ and $C_{25} = 0$, or $C_{14} = 0$ and $C_{25} \neq 0$. For the general trigonal case, one can either specify seven elastic constants, or six elastic constants and the angle of the x axis from the crystalline a axis. For trigonal crystals such as LiKSO_4 , which possess a mirror plane parallel to the c axis, only six elastic constants are needed. These can be taken as the five hexagonal elastic constants and either C_{14} or C_{25} with the angle of the x axis from the a axis as 0° or 90° , respectively.

The elastic constants in the hexagonal phase were determined from the measured frequencies using an iterative method described by Visscher *et al.*³³ and Ohno.⁴¹ The Visscher FORTRAN code was modified for trigonal crystalline symmetry using results of Ohno *et al.*⁴² Approximately 40 frequencies were fit to a set of elastic constants with a typical rms error of 0.16% in the hexagonal phase and 0.35% in the trigonal phase.

The results for the hexagonal and trigonal elastic constants are shown in Figs. 2 and 3. Our room temperature results for the hexagonal elastic constants are in good agreement with previous Brillouin^{22,36} and ultrasonic⁴³ measurements. The present results are in especially good agreement with the recent ultrasonic measurements except for C_{13} where our results are 8% higher; however, C_{13} is especially difficult to determine with conventional ultrasonic techniques. As the figures show, the elastic constants are nearly temperature independent within the hexagonal phase, in agreement with the Brillouin results.²² At 213 K on cooling, all the elastic constants except C_{13} show large changes. On warming from 200 K the elastic constants abruptly return to the high temperature values at 243 K. Our results for C_{66} are in qualitative agreement with those of An *et al.*,²³ although the 80% reduction of C_{66} observed in the present work is much greater than that observed previously. In general our results are in disagreement with those of Mroz *et al.*¹⁶ and Ganot *et al.*¹⁵ who observed no large changes above 200 K for any elastic constants. We observe an increase of about

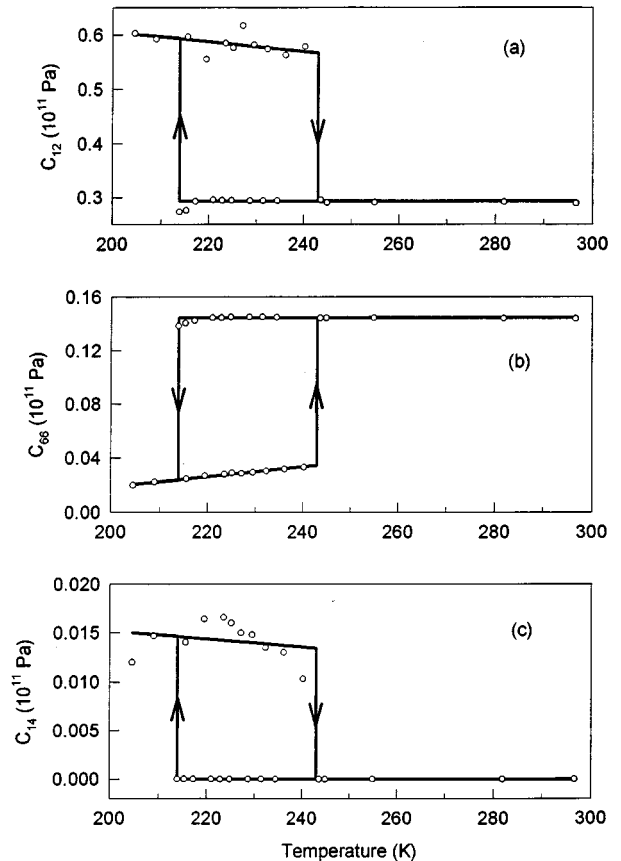


FIG. 2. Elastic constants C_{12} , C_{66} , and C_{14} vs temperature for LiKSO_4 . The circles are the experimental values; the solid lines represent theoretical fits to the data discussed in the text.

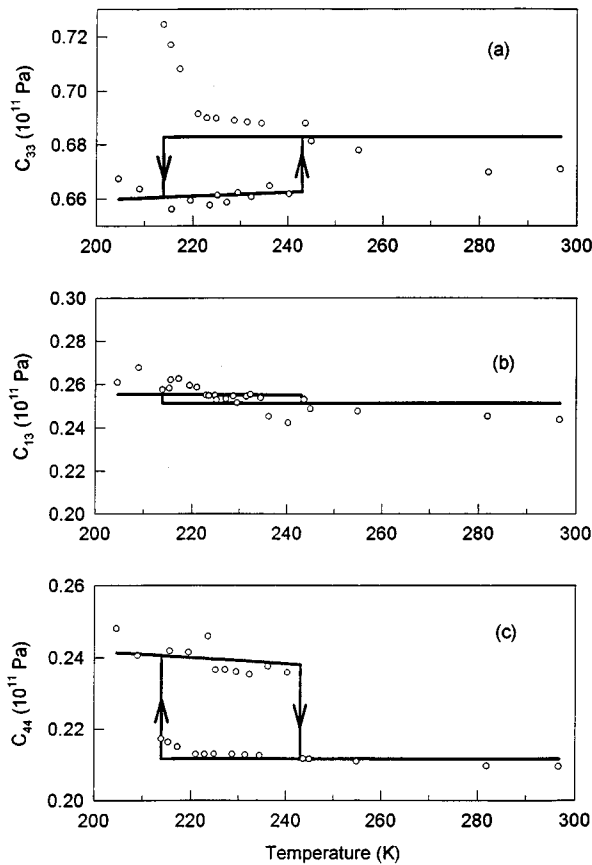


FIG. 3. Elastic constants C_{33} , C_{13} , and C_{44} vs temperature for LiKSO_4 . The circles are the experimental values; the solid lines represent theoretical fits to the data discussed in the text.

10% in C_{11} on entering the trigonal phase, while An *et al.*²³ observed a decrease of about the same magnitude.

The expression for the bulk modulus for both hexagonal and trigonal symmetry can be shown to be

$$B = \frac{C_{33}C_{66} + C_{33}C_{12} - C_{13}^2}{C_{12} - 2C_{13} + C_{33} + C_{66}}. \quad (2)$$

Using the data of Figs. 2 and 3, the bulk modulus was computed. The results are shown in Fig. 4. As can be seen from the figure, the bulk modulus is approximately 15% higher in the trigonal phase than in the hexagonal phase.

To check the sensitivity of RUS to the form of the elastic constant matrix used, data taken at 296 K were analyzed using the trigonal elastic constant code. The values of the elastic constants determined by the hexagonal analysis along with the value of $C_{14} = 0.012 \times 10^{11}$ Pa obtained from analyzing data in the trigonal phase were used as initial values in the computer program. The program was allowed to iterate and the resulting computation of C_{14} and rms error for the overall fit were noted as a function of iteration number. The results are plotted in Fig. 5. As can be seen, C_{14} is driven toward its hexagonal value of zero and the rms error decreases. An attempt was made to analyze data in the trigonal phase using the hexagonal elastic constant matrix. It was not possible to get a good fit to the data. The resulting rms error was approximately 0.8%.

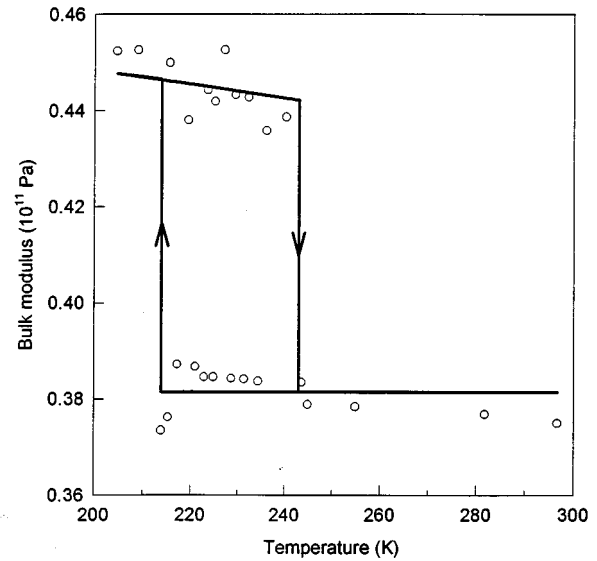


FIG. 4. Bulk modulus vs temperature for LiKSO_4 . The circles represent the data; the solid line represents a fit to the data discussed in the text.

IV. DISCUSSION

A common theory used to treat phase transitions was developed by Landau.⁴⁴ An expansion of the thermodynamic potential for the system is made in a power series of some order parameter, Q . This order parameter is assumed to be some quantity that differentiates the two phases involved. In the original development of the theory, the transition is assumed to occur in such a manner that the crystal always possesses one of two symmetries. The parent phase possesses all the symmetry elements of the daughter phase, plus one or more additional symmetry elements. As long as Q takes on a value of zero, the crystal symmetry is that of the parent phase. As soon as Q takes on any arbitrarily small value, the symmetry is reduced to that of the daughter phase.

Transformations such as the hexagonal/trigonal phase

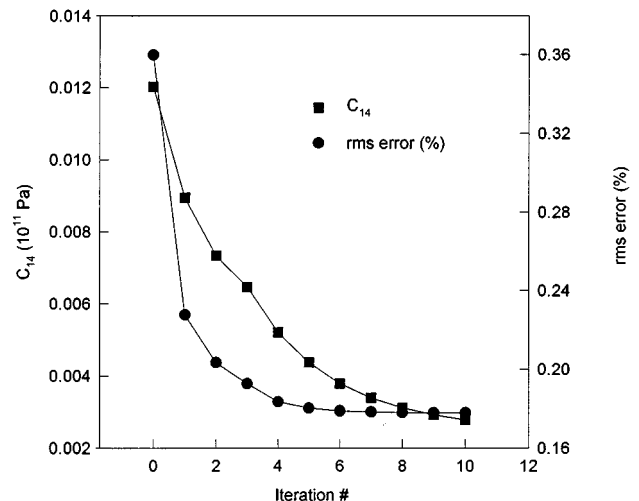


FIG. 5. Values of C_{14} and rms error vs iteration number resulting from using a trigonal elastic constant matrix to fit data in the hexagonal phase.

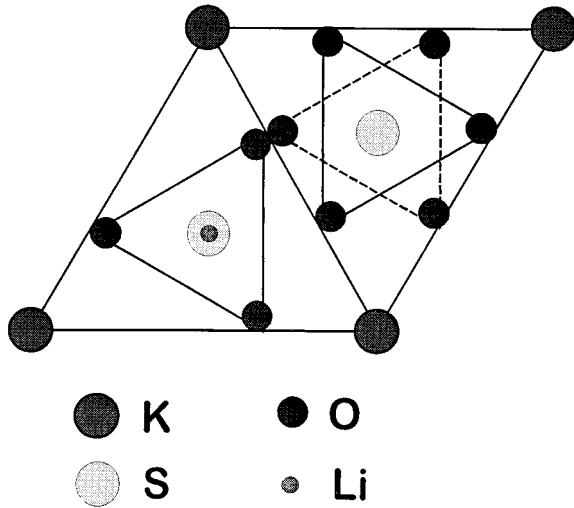


FIG. 6. Illustration of the structure of LiKSO_4 as viewed along the $[001]$ direction. The solid lines represent the hexagonal phase. The dashed lines illustrate the reorientation of one of the SO_4 tetrahedra characterizing the transition to the trigonal phase.

change in LiKSO_4 must be treated differently. The $P6_3$ and the $P31c$ phases do not satisfy a group-subgroup relationship. These transformations are of the reconstructive type.^{45,46} However, it is still possible to make an expansion of the free energy of the two phases in terms of deviations of the order parameter from a parent phase.⁴⁷ We use such an approach for LiKSO_4 . We take the parent phase as hexagonal $P6_3mc$. The $P6_3$ and the $P31c$ phases are subgroups of the $P6_3mc$ phase. The $P6_3mc$ phase apparently does not exist in LiKSO_4 . As the crystal is cooled from high temperatures the sequence of phase transitions is $P6_3/mmc \rightarrow$ modulated phase $\rightarrow P6_3 \rightarrow P31c$. Nevertheless, we can still use $P6_3mc$ as a parent phase from which to expand the free energy.

A drawing emphasizing the differences between the hexagonal and trigonal phases of LiKSO_4 is shown in Fig. 6. The orientations of the SO_4 tetrahedra in the hexagonal phase are represented by the triangles with solid lines. The trigonal phase differs from the hexagonal phase by the rotation of one of the SO_4 tetrahedra as illustrated with the dashed lines on the right. The two SO_4 tetrahedra are displaced from each other by $c/2$ along the c axis. LiKSO_4 transforms from the hexagonal $P6_3$ phase to the trigonal $P31c$ phase when one of the two SO_4 tetrahedra in each unit cell rotates 108° about one of three axes perpendicular to the c axis.^{17,18,36}

We use Fig. 7 to introduce order parameters for this system. One unit cell for each phase is drawn in Fig. 7. Consider the unit cell shown on the lower left for the $P6_3$ phase. We make an arbitrary assignment of s_1 to the left SO_4 tetrahedron (A) and s_2 to the right SO_4 tetrahedron (B) in that unit cell. If the SO_4 tetrahedron is found oriented such as A, we assign its s a value of $+1$. If the SO_4 tetrahedron is found oriented such as B, we assign its s a value of -1 . These two orientations differ only by a rotation of the SO_4 tetrahedron about an axis in the basal plane. We now let the two individual s be the difference in the probability of finding the SO_4 tetrahedron in the two states ($s_k \equiv P_{kA} - P_{kB}$). If the unit cell has a larger probability of having a SO_4 tetrahedron as

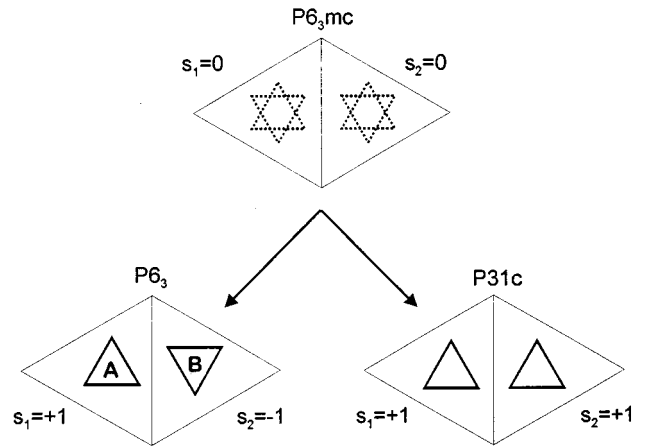


FIG. 7. Diagram showing the relationship between the crystal-line phases and order parameters. The $P6_3$ and the $P31c$ phases are described in terms of a prototypical $P6_3mc$ phase. The orientations of the SO_4 tetrahedra are described by the parameters s_1 and s_2 where the subscripts 1 and 2 correspond to the two sides of the unit cell as shown. The values $+1$ and -1 correspond to the orientations illustrated.

A, the s for that SO_4 tetrahedron would be greater than zero. Likewise, if a SO_4 tetrahedron has a higher probability of being found as B, its s would be less than zero. As the value of s approaches zero, there would be an equal probability of finding the SO_4 tetrahedron in either state. This case of $s_1 = s_2 = 0$ is represented by the dashed lines in the unit cell corresponding to the $P6_3mc$ phase. To differentiate between the two phases, it is easy to see in Fig. 7 that the two s will have different signs in the hexagonal phase (antiparallel), and the same sign in the trigonal phase (parallel). Therefore, for convenience, we define two order parameters as $Q_1 = (s_1 - s_2)/2$ and $Q_2 = (s_1 + s_2)/2$. The hexagonal phase is then specified by $(Q_1, Q_2) = (\pm x, 0)$ and the trigonal phase is specified by $(Q_1, Q_2) = (0, \pm y)$. The $P6_3mc$ phase would correspond to $(Q_1, Q_2) = (0, 0)$. This phase might be expected at sufficiently high temperatures, but is not observed. A modulated phase is observed instead.

The free energy expansion for systems with two coupled order parameters has been described by Imry.⁴⁸ For the present case, we expand the free energy in terms of Q_1 and Q_2 and include coupling between these two order parameters and coupling between the order parameters and the strain e ,

$$F_L(Q_1, Q_2, e_i) = a_1 Q_1^2 + \frac{1}{2} b_1 Q_1^4 + a_2 Q_2^2 + \frac{1}{2} b_2 Q_2^4 + \lambda Q_1^2 Q_2^2 + F_c(Q_1, Q_2, e_i) + \frac{1}{2} \sum_{i,j} C_{ij} e_i e_j, \quad (3)$$

where a_i and b_i are the usual Landau expansion coefficients and λ characterizes the strength of the coupling between the two order parameters. $F_c(\mathbf{Q}, \mathbf{e})$ describes the coupling between the order parameters and the strains. The last term represents the usual elastic energy. Imry⁴⁸ shows that for $\lambda > (b_1 b_2)^{1/2}$ Eq. (3) describes a first-order phase transition, which is of interest for LiKSO_4 .

The effect on the elastic constants due to coupling between the strains and the order parameters can be shown to be^{49,50}

$$C'_{mn} = C_{mn} + \frac{\partial^2 F_c}{\partial e_m \partial e_n} \sum_{k,l} \left(\frac{\partial^2 F}{\partial Q_k \partial e_m} \right) \times \left(\frac{\partial^2 F}{\partial Q_k \partial Q_l} \right)^{-1} \left(\frac{\partial^2 F}{\partial e_n \partial Q_l} \right). \quad (4)$$

We now invoke symmetry arguments to constrain the form of $F_c(\mathbf{Q}, \mathbf{e})$. As discussed above, reversal of either Q_1 or Q_2 will not change the symmetry of the crystal. Thus the free energy must be invariant under the reversal of the sign of either Q_1 or Q_2 . $F_c(\mathbf{Q}, \mathbf{e})$ must then be of the form

$$F_c(Q_1, Q_2, e) = F_{1c}(Q_1, Q_2, e_i) + F_{2c}(Q_1, Q_2, e_i), \quad (5)$$

with

$$F_{1c}(Q_1, Q_2, e_i) = Q_1^2 \sum_i k_{1i} e_i + Q_2^2 \sum_i k_{2i} e_i, \\ F_{2c}(Q_1, Q_2, e_i) = \frac{Q_1^2}{2} \sum_{i,j} k_{1ij} e_i e_j + \frac{Q_2^2}{2} \sum_{i,j} k_{2ij} e_i e_j \quad (6)$$

and possible higher order terms in Q and e . The sums in Eq. (6) run over the six strains $e_1 \dots e_6$.

The free energy must be invariant under the symmetry operations of the crystal. Because the order parameter we have chosen is a scalar it is automatically invariant. The form of the elastic constant matrix, C_{ij} , assures that the elastic energy is invariant. It only remains to examine $F_c(\mathbf{Q}, \mathbf{e})$. $F_{2c}(\mathbf{Q}, \mathbf{e})$, coupling quadratic in the strain, has the same form as the elastic energy. This term will be invariant if k_{1ij} and k_{2ij} have the form of the elastic constant matrix. We now examine $F_{1c}(\mathbf{Q}, \mathbf{e})$ which involves coupling linear in the strain. We require invariance under a rotation of $2\pi/3$ about the c axis. Carrying out this transformation⁴⁰ shows that the terms linear in the strain must be of the form

$$F_{1c}(Q_1, Q_2, e_i) = k_{11} Q_1^2 (e_1 + e_2) + k_{13} Q_1^2 e_3 + k_{21} Q_2^2 (e_1 + e_2) + k_{23} Q_2^2 e_3 \quad (7)$$

in order that $F_{1c}(\mathbf{Q}, \mathbf{e})$ be invariant under the symmetry operations of $P31c$. This form is also invariant under the operations of $P6_3$.

Using Eq. (7) in Eq. (4) shows that, at the transition, the changes in C_{11} and C_{12} are identical. The only other predicted changes are for C_{33} and C_{13} , all other elastic constants are predicted to have zero changes at the transition, including C_{66} . These predictions are in strong disagreement with the experimental results. In addition we observe no change in C_{13} which requires at least one of the coupling coefficients in Eq. (7) to vanish for each phase leading to $\Delta C_{12} = \Delta C_{11} = 0$, or $\Delta C_{33} = 0$. This follows from applying Eq. (4) to Eqs. (3) and (7). The change in C_{13} is proportional to $k_{11} k_{13}$ in the hexagonal phase and $k_{21} k_{23}$ in the trigonal phase. No change in C_{13} thus requires one of the two constants be zero in each phase, resulting in no change in C_{11} and C_{12} , or no change in C_{33} . Thus we conclude that coupling linear in the strain cannot explain the experimental results.

We now proceed with coupling quadratic in the strain. Using the $F_{2c}(\mathbf{Q}, \mathbf{e})$ of Eq. (6) in Eq. (4), it is easy to see that the effects of the coupling between the order parameters and strains on the elastic constants in the hexagonal and trigonal phases are

$$C_{mn}^{(\text{hex})} = C_{mn} + k_{1mn} Q_1^2, \\ C_{mn}^{(\text{trig})} = C_{mn} + k_{2mn} Q_2^2. \quad (8)$$

As discussed above, k_{1mn} has the form of the elastic constant matrix for hexagonal symmetry while k_{2mn} has the form of the elastic constant matrix for trigonal symmetry. Thus bi-quadratic coupling of the order parameters and strains permits a change in the entire set of elastic constants at the phase transition.

We now examine the nature of the phase transition described by the free energy expansion of Eq. (3). In the usual Landau theory with a single order parameter, a phase transition is obtained by letting the coefficient of the quadratic term change sign at some temperature. A minimum exists at $Q=0$ for high temperatures, when the sign of the quadratic term is positive. As the temperature drops below some critical value, the sign of the quadratic term becomes negative and the minimum moves away from the origin to a nonzero value of Q . The two phases are distinguished by $Q=0$ in the higher symmetry phase and $Q \neq 0$ in a lower symmetry phase.

The present situation with two order parameters which are coupled is more complicated. Imry⁴⁸ describes in detail the phase diagram of a system with two order parameters such as that in Eq. (3). With two order parameters, there exists the possibility that two terms can change signs. As in the case of a second order transition described by a single order parameter, the high temperature phase of a two order parameter system exists with a single minimum found at the origin of Q space, with $Q_1 = Q_2 = 0$ and both a_1 and a_2 positive. As the temperature falls below some value T_1 , a second order transition occurs as the minimum moves out along the Q_1 axis. This occurs when the sign of a_1 changes from positive to negative while a_2 remains positive. Following Landau⁴⁴ and Imry,⁴⁸ we let the sign of a_1 change by including only a linear term for its temperature dependence as in Eq. (9),

$$a_1 = \frac{\alpha_1(T - T_1)}{T_1}, \quad (9)$$

with α_1 and T_1 constants. The value of Q_1 at the minimum is given by

$$Q_1^2 = -\frac{a_1}{b_1}. \quad (10)$$

The minimum that develops along the Q_1 axis deepens and continues to move to larger values of Q_1 as the temperature decreases. If only a_1 is allowed to change sign, only this one transition can occur, despite having two order parameters. In order for more interesting changes to occur, we must also let

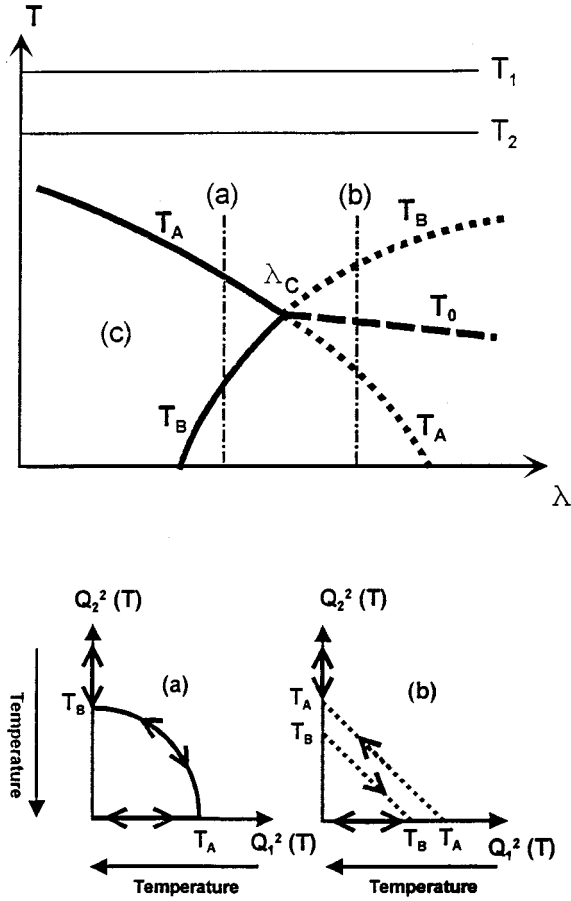


FIG. 8. Two types of phase transitions can develop in systems with biquadratic coupling between two order parameters depending on the strength of the coupling. Weak coupling ($\lambda < \lambda_c$) is shown in (a) and strong coupling ($\lambda > \lambda_c$) is shown in (b). The two vertical lines in (c) correspond to the temperature dependencies shown in (a) and (b), respectively.

a_2 change sign at some temperature, T_2 . Once again, we choose the simplest means to let a_2 change sign, as was done for a_1 in Eq. (9).

There are two different types of phases diagrams possible depending on the strength of the coupling between the order parameters as shown in Fig. 8. If the coupling is weak, $\lambda < (b_1 b_2)^{1/2}$, three second order transitions occur. The first occurs as described above. The second occurs as the minimum moves off the Q_1 axis to a phase with both order parameters having nonzero values. The minimum then moves through Q space to the Q_2 axis. A third continuous transition occurs as the system undergoes a transformation to a phase corresponding to a minimum along the Q_2 axis. If the coupling is strong, $\lambda > (b_1 b_2)^{1/2}$, a second-order and a first-order transition occur. The second-order transition is as described above when the system moves away from $Q_1 = Q_2 = 0$. The first-order transition, which is of interest for LiKSO_4 , will be treated in more detail below.

Simply letting a_2 change sign at T_2 does not immediately create additional minima for either type of coupling. For strong coupling, the minimum along the Q_1 axis continues to be the only minimum until the temperature drops below T_B given by the solution of

$$\lambda = \frac{a_1 b_2}{a_2}. \quad (11)$$

Below this temperature, a second minima develops along the Q_2 axis, but is energetically unfavorable. As the temperature continues to decrease, the difference in the value of the free energy at the two minima decreases. Eventually a temperature, T_0 , is reached at which the free energies at the two minima are equal. For temperatures below T_0 , the free energy at the minimum along the Q_2 axis is lower than the free energy at the Q_1 minimum, but a potential barrier prevents the system from changing states. The system continues to remain in the state corresponding to a nonzero value of Q_1 until the height of the barrier becomes small enough and the difference of the free energy becomes great enough that a first-order phase transition occurs. This is the observed transition temperature on cooling and two minima will likely exist for a finite temperature interval below the observed transition temperature. As the temperature continues to decrease, the minimum along the Q_1 axis becomes a saddle point at T_A , given by the solution of

$$\lambda = \frac{a_2 b_1}{a_1}. \quad (12)$$

The temperature range from T_A to T_B is often referred to as the coexistence region and these temperatures are the limits between which two minima exist. The temperature dependence as the system is warmed from below T_A is exactly the same as during cooling with the roles of Q_1 and Q_2 reversed. The system starts at low temperatures in a phase with a nonzero value of Q_2 . The minimum along the Q_2 axis moves in towards the origin as the temperature increases. As the temperature warms to a value above T_A given by the solution of Eq. (12), the second minima develops along the Q_1 axis. The system remains in the low temperature phase until changing discontinuously back to the phase along the Q_1 axis at a temperature $\leq T_B$.

It was experimentally observed during the measurements reported here that there is only a slight temperature dependence of the elastic constants in the hexagonal region. The slight changes are no more than what one normally expects as a material is cooled. Therefore, we choose to ignore any temperature dependence of the Q_1 order parameter, corresponding to the hexagonal phase and take a_1 to be a negative constant. This situation could be interpreted as $T_1 \gg T$ for the temperature range of our measurements. We do observe a larger than normal temperature dependence for the elastic constants in the trigonal phase, so we let a_2 have the temperature dependence specified above. The behavior of the elastic constants are then given by

$$C_{mn}^{(\text{hex})} = C_{mn} - \frac{k_{1mn} a_1}{b_1} = C'_{mn} = \text{const}, \quad (13)$$

$$C_{mn}^{(\text{trig})} = C_{mn} + \frac{k_{2mn} \alpha_2}{b_2} \left(1 - \frac{T}{T_2} \right) = C''_{mn} - k'_{2mn} T.$$

We then see that all the elastic constants must have the same temperature dependence, the magnitude and direction of the step at the transition being the only difference. The expressions for T_A and T_B now reduce to

$$T_A = T_2 \left(1 + \frac{a_1 \lambda}{\alpha_2 b_1} \right), \quad T_B = T_2 \left(1 + \frac{a_1 b_2}{\alpha_2 \lambda} \right). \quad (14)$$

The elastic constants determined from measurement by RUS are plotted in Figs. 2 and 3 along with the fit of Eqs. (13). As can be seen, there is excellent agreement between the fits to C_{66} and C_{12} and the data obtained. Fits between theory and data for the other elastic constants are within the uncertainties in the measurements. The constants determined from fitting Eqs. (13) to the data were used to calculate the bulk modulus using Eq. (2). The result is shown as the solid line in Fig. 4.

The vertical lines with arrows are drawn at the temperatures at which the transitions were seen to occur. These vertical lines are probably not at exactly the temperatures T_A and T_B . As mentioned above, T_A and T_B are the limits of stability; the hexagonal phase can exist down to T_A and the trigonal phase can exist up to T_B . We do not have enough information to calculate T_A and T_B from Eqs. (14). The observed transition temperatures indicate that $T_B - T_A \geq 30$ K.

V. CONCLUSIONS

Using resonant ultrasound spectroscopy, the complete set of elastic constants for single-crystal LiKSO_4 has been measured in the temperature region of 200 to 300 K including both the hexagonal and trigonal phases. The values of the elastic constants in the room temperature hexagonal phase are in excellent agreement with earlier results. Large step changes in all elastic constants except C_{13} are observed at the hexagonal-trigonal transition. For example, C_{66} drops to 15% of its hexagonal value on entering the trigonal phase. The bulk modulus is about 15% higher in the trigonal phase than in the hexagonal phase. A large hysteresis is observed; the abrupt change in elastic constants occurs about 30 K

higher on warming than on cooling. The transitions were found to be very sluggish, taking hours to equilibrate.

The changes of the elastic constants at the phase transition are explained in terms of a Landau-type expansion of the free energy. Two Ising-like order parameters with strong, biquadratic coupling between the parameters accounts for the first-order nature of the transition including the hysteresis. The symmetry of the crystal is compatible with either an order parameter-strain coupling which is quadratic in the order parameters and linear in the strains, or a coupling biquadratic in the order parameters and the strains. However, the quadratic-linear order parameter-strain coupling permits changes in only C_{11} , C_{12} , C_{13} , and C_{33} whereas large changes were observed in all elastic constants except C_{13} ; especially large changes were observed in C_{66} for which quadratic-linear coupling predicts no change at the transition. The biquadratic order parameter-strain coupling permits step changes in all the elastic constants at the transition and hence is in agreement with the experimental results. The temperature dependence of the elastic constants in the trigonal phase is accounted for by the model.

Data in the room temperature phase are fit well with a hexagonal form of the elastic constant matrix. An attempt to fit the data in this phase with a trigonal elastic constant matrix resulted in C_{14} being driven toward zero. Data in the lower temperature phase required using a nonzero value for C_{14} to obtain a good fit. Our data thus support the phase occurring below 213 K as trigonal.

ACKNOWLEDGMENTS

We are indebted to Dr. M. P. Gelfand for helpful suggestions. One of the authors (T.K.) wishes to express his thanks to Dr. K. Nobugai of Osaka University for supplying the crystal. This work was supported by the National Science Foundation under Grant No. DMR-9501550.

- ¹A. Lunden and J. O. Thomas, in *High Conductivity Solid Ionic Conductors: Recent Trends and Applications*, edited by T. Takahashi (World Scientific, Singapore, 1986).
- ²A. Lunden and L. Nilsson, *J. Mater. Sci. Lett.* **5**, 645 (1986).
- ³A. J. Bradley, *Philos. Mag.* **45**, 1225 (1925).
- ⁴N. Choudhury, S. L. Chaplot, and K. R. Rao, *Phys. Rev. B* **33**, 8607 (1986).
- ⁵M. Drozdowski and F. Holuj, *Ferroelectrics* **77**, 47 (1988).
- ⁶H. Kabelka and G. Kuchler, *Ferroelectrics* **88**, 93 (1988).
- ⁷A. J. Oliveira, F. A. Germano, J. Mendes-Filho, F. E. A. Melo, and J. E. Moreira, *Phys. Rev. B* **38**, 12 633 (1988).
- ⁸H. Bill, Y. Ravi Sekhar, and D. Lovy, *J. Phys. C* **21**, 2795 (1989).
- ⁹M. A. Pimenta, P. Echegut, Y. Luspain, G. Hauret, F. Gervais, and P. Abékard, *Phys. Rev. B* **39**, 3361 (1989).
- ¹⁰G. J. Perpetuo, M. S. S. Dantas, R. Gazzinello, and M. A. Pimenta, *Phys. Rev. B* **45**, 5163 (1992).
- ¹¹A. Desert, A. Gibaud, A. Righi, U. A. Leitão, and R. L. Moreira, *J. Phys. Condens. Matter* **7**, 8445 (1995).
- ¹²Jiang-Tsu and Shen Yuan Chou, *J. Phys. Chem. Solids* **47**, 1171 (1986).
- ¹³S. Bhakay-Tamhane, A. Sequeira, and R. Chidambaram, *Solid State Commun.* **53**, 197 (1985).
- ¹⁴H. Rajagopal, Victor Jaya, A. Sequeira, and R. Chidambaram, *Physica B* **174**, 95 (1991).
- ¹⁵F. Ganot, B. Kihal, R. Farhi, and P. Moch, *Jpn. J. Appl. Phys.* **24**, Suppl. 24-2, 491 (1985).
- ¹⁶B. Mroz, J. A. Tuszynski, H. Kieft, and M. J. Clouter, *J. Phys. Condens. Matter* **1**, 5965 (1989).
- ¹⁷S. L. Chaplot, K. R. Rao, and A. P. Roy, *Phys. Rev. B* **29**, 4747 (1984).
- ¹⁸M. L. Bansal and A. P. Roy, *Phys. Rev. B* **30**, 7307 (1984).
- ¹⁹S. Shin, Y. Tezuka, and A. Sugawara, *Phys. Rev. B* **44**, 11 724 (1991).
- ²⁰R. C. de Sousa, J. A. C. Paiva, J. Mendes Filho, and A. Sergio Bezerra Sombra, *Solid State Commun.* **87**, 959 (1993).
- ²¹U. A. Leitão, A. Righi, P. Bourson, and M. A. Pimenta, *Phys. Rev. B* **50**, 2754 (1994).
- ²²B. Mroz, T. Krajewski, T. Breczewski, W. Chomka, and D. Sematowicz, *Ferroelectrics* **42**, 71 (1982).
- ²³T. An, L. Ling-qing, G. Ben-yuen, M. Yu-jun, Y. Hua-quang, and W. Yan-yun, *Solid State Commun.* **61**, 1 (1987).
- ²⁴J. A. Krumhansl, *Solid State Commun.* **84**, 251 (1992).
- ²⁵C. W. Garland, in *Physical Acoustics VII*, edited by W. P. Warren and R. N. Thurston (Academic, New York, 1970).

- ²⁶R. L. Melcher, in *Physical Acoustics Vol. XII*, edited by W. P. Warren and R. N. Thurston (Academic, New York, 1976).
- ²⁷D. J. Gunton and G. A. Saunders, *Solid State Commun.* **14**, 865 (1974).
- ²⁸Y. Gefen and M. Rosen, *Philos. Mag.* **26**, 727 (1972).
- ²⁹N. G. Page and G. A. Saunders, *Proc. R. Soc. London Ser. A* **326**, 521 (1972).
- ³⁰S. Kashida and H. Kaga, *J. Phys. Soc. Jpn.* **42**, 499 (1977).
- ³¹R. D. Lowde, R. T. Harley, G. A. Saunders, M. Sato, R. Scherm, and C. Underhill, *Proc. R. Soc. London Ser. A* **374**, 87 (1981).
- ³²G. A. Kneezel and A. V. Granato, *J. Phys. (Paris) Colloq.* **42**, C5-1061 (1981).
- ³³W. M. Visscher, A. Migliori, T. M. Bell, and R. A. Reinert, *J. Acoust. Soc. Am.* **90**, 2154 (1991).
- ³⁴J. D. Maynard, *J. Acoust. Soc. Am.* **91**, 1754 (1992).
- ³⁵A. Migliori, J. L. Sarrao, W. M. Visscher, T. M. Bell, Ming Lei, Z. Fisk, and R. G. Leisure, *Physica B* **183**, 1 (1993).
- ³⁶M. A. Pimenta, Y. Luspín, and G. Hauret, *Solid State Commun.* **59**, 481 (1986).
- ³⁷R. Holland, *J. Acoust. Soc. Am.* **43**, 988 (1968).
- ³⁸H. H. Demarest, *J. Acoust. Soc. Am.* **49**, 768 (1971).
- ³⁹O. L. Anderson, E. Schreiber, and N. Soga, *Elastic Constants and Their Measurements* (McGraw-Hill, New York, 1973).
- ⁴⁰Fedor I. Federov, *Theory of Elastic Waves in Crystals* (Plenum, New York, 1968).
- ⁴¹Ichiro Ohno, *J. Phys. Earth* **24**, 355 (1976).
- ⁴²Ichiro Ohno, Shigeru Yamamoto, Orson L. Anderson, and Jiro Noda, *J. Phys. Chem. Solids* **47**, 1103 (1986).
- ⁴³L. Godfrey and J. Philip, *Solid State Commun.* **97**, 635 (1996).
- ⁴⁴L. D. Landau and E. M. Lifshitz, *Statistical Physics* (Pergamon, New York, 1980).
- ⁴⁵W. D. Kingery, H. K. Bowen, and D. R. Uhlmann, *Introduction to Ceramics* (Wiley, New York, 1976).
- ⁴⁶Jean-Claude Tolédano and Pierre Tolédano, *The Landau Theory of Phase Transitions* (World Scientific, Singapore, 1987).
- ⁴⁷E. K. H. Salje, *Phase Transitions in Ferroelastic and Co-Elastic Crystals* (Cambridge University Press, Cambridge, England, 1990).
- ⁴⁸Joseph Imry, *J. Phys. C* **8**, 567 (1975).
- ⁴⁹J. C. Slonczewski and H. Thomas, *Phys. Rev. B* **1**, 3545 (1970).
- ⁵⁰Walter L. Rehwald, *Adv. Phys.* **22**, 721 (1973).